ELSEVIER

Physics Reports 242 (1994) 5–35

PHYSICS REPORTS

Nucleon–nucleon potentials in comparison: Physics or polemics?†

R. Machleidt[1,*], G.Q. Li

Department of Physics, University of Idaho, Moscow, ID 83843, USA

Abstract

Guided by history, we review the major developments concerning realistic nucleon–nucleon (NN) potentials since the pioneering work by Kuo and Brown on the effective nuclear interaction. Our main emphasis is on the physics underlying various models for the NN interaction developed over the past quarter-century. We comment briefly on how to test the quantitative nature of nuclear potentials properly. A correct calculation (performed by independent researchers) of the χ^2/datum for the fit of the world NN data yields 5.1, 3.7, and 1.9 for the Nijmegen, Paris, and Bonn potential, respectively. Finally, we also discuss in detail the relevance of the on- and off-shell properties of NN potentials for microscopic nuclear structure calculations.

1. Introduction

To most of us, Tom Kuo is best known for this seminal work on the effective interaction of two valence nucleons in nuclei ('Kuo–Brown matrix elements') published in 1966 [1]. One of the most fundamental goals of theoretical nuclear physics is to understand atomic nuclei in terms of the basic nucleon–nucleon (NN) interaction. Tom and Gerry's work of 1966 was the first successful step towards this goal. Microscopic nuclear structure has essentially two ingredients: many-body theory and the nuclear potential. During the past 25 years, there has been progress in both of these fields. Tom Kuo has worked consistently on the improvement of the many-body approaches appropriate for nuclear structure problems [2,3]. On the other hand, there have also been substantial advances in our understanding of the NN interaction since 1966, when the Hamada–Johnston potential [4] was the only available quantitative NN potential.

Therefore, we are happy to take this opportunity to give an overview of the progress made in the field of realistic two-nucleon potentials in the past quarter-century. It is not our intention to

* Corresponding author.

† Dedicated to Tom Kuo on the occasion of his 60th birthday.

[1] Invited talk presented at 'Realistic Nuclear Structure', a conference to mark the 60th Birthday of T.T.S. Kuo, May 1992, Stony Brook, NY.

SSDI 0370-1573(94)00007-P

mention and analyse all NN potentials that have appeared on the market ever since the work of Hamada–Johnston [4] and Reid [5].[2] Here, our focus will be on the underlying physics of realistic models for the nuclear potential. Most transparently, this physics has evolved in three stages, and we will give essentially only one representative example for each stage (Section 2).

We do so to avoid confusing the reader with too many technical details that may distract from the interesting physics involved. However, for reasons of fairness, we like to stress that our sub-selection is essentially accidental, and that there are many other, equally representative examples for each stage of the development of theoretical nuclear potentials. In particular, we mention the potential by Tourreil et al. [7], the Argonne V_{14} potential [8], and the more recent models developed at Bochum [9], Williamsburg [10], and Hamburg [11].

With an eye on the topic of this conference, we like to restrict our review to quantitative NN potentials suitable for application in nuclear structure. Therefore, we will not discuss the numerous and interesting recent attempts of deriving the NN interaction from models for low-energy QCD.

For microscopic nuclear structure work, it is important that the NN potential applied is able to reproduce the known facts about the two-nucleon system correctly. Therefore, in Section 3, we will make some comments on how to test the quantitative nature of a two-nucleon potential properly. Most relevant for this conference is the question to which extent nuclear structure results depend on the kind of potential used as input in the calculations. We will discuss this in Section 4. Our contribution finishes with summary and conclusions given in Section 5.

2. Physics

The underlying physics of different meson-theory based models for the NN interaction will be explained in this section. This is done most clearly by following the historical path.

2.1. The one-boson-exchange model and the Nijmegen potential

The first quantitative meson-theoretic models for the NN interaction were the one-boson-exchange potentials (OBEP). They emerged after the experimental discovery of heavy mesons in the early 1960s. In general, about six nonstrange bosons with masses below 1 GeV are taken into account (cf. Fig. 1): the pseudoscalar mesons $\pi(138)$ and $\eta(549)$, the vector mesons $\rho(769)$ and $\omega(783)$, and two scalar bosons $\delta(983)$ and $\sigma(\approx 550)$. The first particle in each group is isovector while the second is isoscalar. The pion provides the tensor force, which is reduced at short range by the ρ meson. The ω creates the spin-orbit force and the short-range repulsion, and the σ is responsible for the intermediate-range attraction. Thus, it is easy to understand why a model which includes the above four mesons can reproduce the major properties of the nuclear force.[3]

A classic example for an OBEP is the Bryan–Scott (B–S) potential published in 1969 [12]. Since it is suggestive to think of a potential as a function of r (where r denotes the distance between the centers of the two interacting nucleons), the OBEPs of the 1960s were represented as local r-space

[2] A more detailed account of this can be found in Section 2 of Ref. [6].

[3] The interested reader can find a detailed and pedagogical introduction into the OBE model in [6, Sections 3, 4].

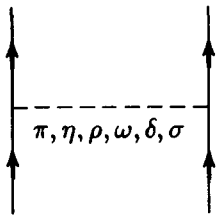

Fig. 1. One-boson-exchange (OBE) model for the NN interaction.

potentials. To reduce the original one-meson-exchange Feynman amplitudes to such a simple form, drastic approximations have to be applied. The usual method is to expand the amplitude in terms of p^2/M and keep only terms up to first-order (and, in many cases, not even all of them). Commonly, this is called the *nonrelativistic* OBEP. Besides the suggestive character of a local function of r, such potentials are easy to apply in r-space calculations. However, the original potential (Feynman amplitudes) is nonlocal, and, thus, has a very different off-shell behavior than its local approximation. Though this does not play a great role in two-nucleon scattering, it becomes important when the potential is applied to the nuclear few- and many-body problems. In fact, it turns out that the original nonlocal potential leads to much better predictions in nuclear structure than the local approximation. We will discuss this in detail in Section 4.

Historically, one must understand that after the failure of the pion theories in the 1950s, the one-boson-exchange (OBE) model was considered a great success in the 1960s. However, there are conceptual and quantitative problems with this model.

A principal deficiency of the OBE model is the fact that it has to introduce a scalar-isoscalar σ-boson in the mass range 500–700 MeV, the existence of which is not supported by any experimental evidence. Furthermore, the model is restricted to single exchanges of bosons that are 'laddered' in an unitarizing equation. Thus, irreducible multi-meson exchanges, which may be quite sizable (see below), are neglected.

Quantitatively, a major drawback of the *nonrelativistic* OBE model is its failure to describe certain partial waves correctly. In Figs. 2(a) and (b), we show phase shifts for the $^1P_1$ and $^3D_2$ state, respectively. It is clearly seen that the Bryan–Scott nonrelativistic OBE potential (B–S, long dashes) predicts these phases substantially above the data.

An important progress of the 1970s has been the development of the *relativistic* OBEP [17]. In this model, the full, relativistic Feynmann amplitudes for the various one-boson-exchanges are used to define the potential. These nonlocal expressions do not pose any numerical problems when used in momentum space[4]. The quantitative deficiencies of the nonrelativistic OBEP disappear immediately when the nonsimplified, relativistic, nonlocal OBE amplitudes are used.

The *Nijmegen potential* [13], published in 1978, is a nonrelativistic r-space OBEP. As a late representative of this model, it is one of the most sophisticated examples of its kind. It includes all nonstrange mesons of the pseudoscalar, vector, and scalar nonet. Thus, besides the six mesons

[4] In fact, in momentum space, the application of a nonlocal potential is numerically as easy as using the momentum-space representation of a local potential.

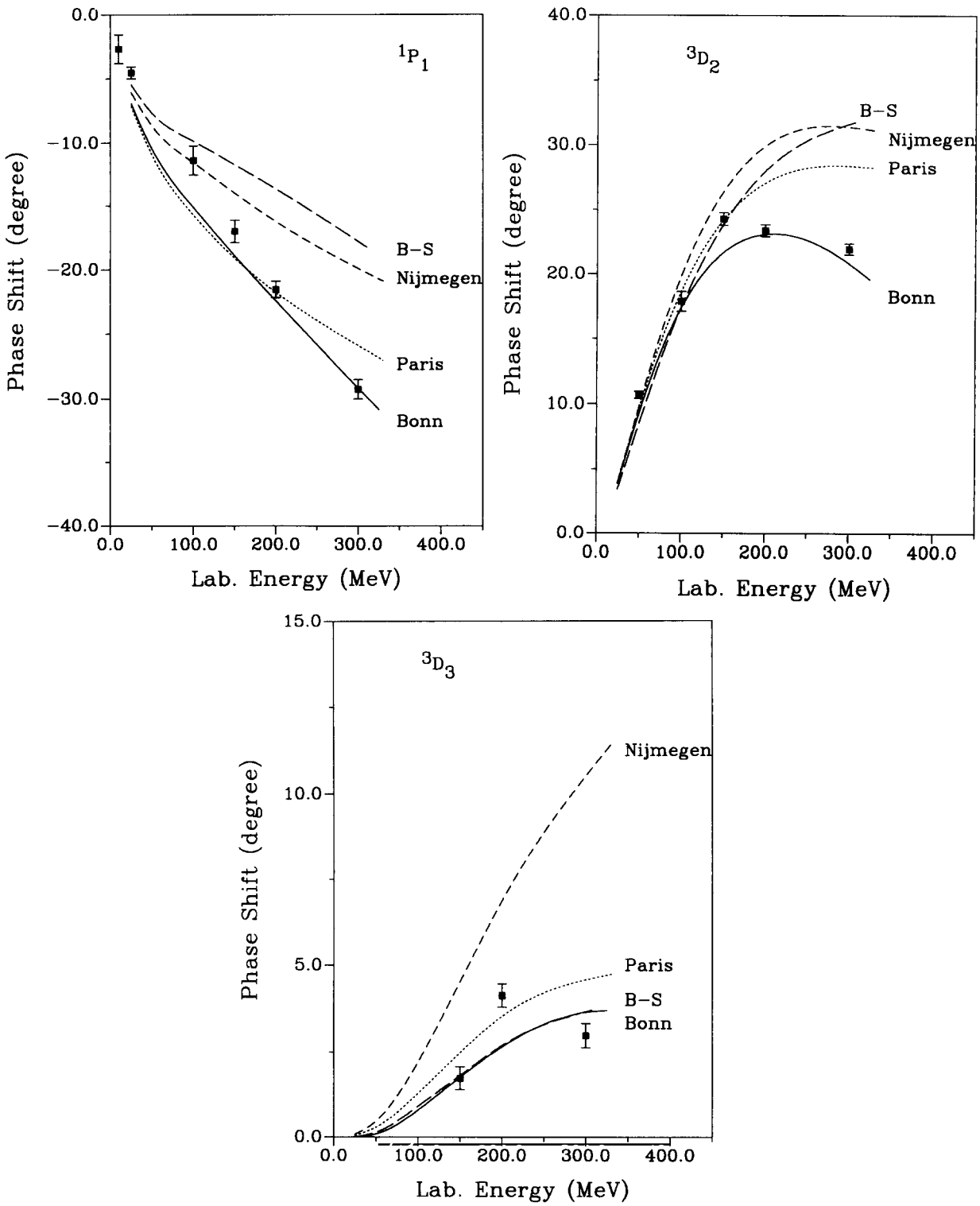

Fig. 2. Phase-shifts of NN scattering for the (a) $^1P_1$, (b) $^3D_2$, and (c) $^3D_3$ partial wave. Predictions are shown for the Bryan–Scott (B–S) potential of 1969 [12] (long dashes), Nijmegen potential [13] (short dashes), Paris potential [14] (dotted), and the Bonn full model [15] (solid line). The solid squares represent the energy-independent phase shift analysis by Arndt et al. [16].

mentioned above, the $\eta'(958)$, $\phi(1020)$, and S*(993) are taken into account. The model also includes the dominant $J = 0$ parts of the Pomeron and tensor (f, f', A_2) trajectories, which essentially lead to repulsive central Gaussian potentials. For the pomeron (which from today's point of view may be considered as a multi-gluon exchange) a mass of 308 MeV is assumed. At the meson–nucleon vertices, a cutoff (form factor) of exponential shape is applied (most OBEP use cutoffs of monopole type). However, this potential is still defined in terms of the nonrelativistic local approximations to the OBE amplitudes. Therefore, it shows exactly the same problems as its ten years older counterpart, the Bryan–Scott potential (cf. Fig. 2): the Nijmegen potential fails to predict the $^1P_1$ and $^3D_2$ phase shifts correctly almost to the same extent as the Bryan–Scott potential. In addition, the Nijmegen potential overpredicts the $^3D_3$ phase shifts by more than a factor of two (Fig. 2(c)), a problem the models of the 1960s did not have. The inclusion of more bosons did obviously not improve the fit of the data. In fact, in the case of the $^3D_3$, there is a dramatic deterioration as compared to earlier models (cf. Fig. 2(c)).

Spin observables of neutron–proton scattering are quite sensitive to the $^3D_2$ and $^3D_3$ partial waves. Therefore, a quantitative description of these waves is important. In Fig. 3 we show the spin correlation parameter C_{NN} at 181 MeV as measured at the Indiana Cyclotron [18] and at 220 MeV with the data from TRIUMF [19]. Failures to reproduce this observable can be clearly traced to the $^3D_2$ and $^3D_3$ (cf. Figs. 2(b) and (c)).

2.2. *The 2π-exchange and the Paris potential*

In the 1970s, work on the meson theory of the nuclear force focused on the 2π-exchange contribution to the NN interaction to replace the fictitious σ-boson. One way to calculate these contributions is by means of dispersion relations (Fig. 4). In this approach, one assumes that the total 2π-exchange contribution to the NN interaction, Fig. 4(a), can be analysed in terms of two 'halves' (Fig. 4(b)). The hatched oval stands for all possible processes involving a pion and a nucleon. More explicitly, this is shown in Figs. 4(c)–(e). The amplitude Fig. 4(c) is calculated from empirical input of πN and ππ scattering. Around 1970, many groups throughout the world were involved in this approach; we mention here, in particular, the Stony Brook [20] and the Paris group [21]. These groups could show that the intermediate-range part of the nuclear force is, indeed, described correctly by the 2π-exchange as obtained from dispersion integrals (see Fig. 7, below).

To construct a complete potential, the Stony Brook as well as the Paris group complemented their 2π-exchange contribution by one-pion-exchange (OPE) and ω-exchange. In addition to this, the Paris potential contains a phenomenological short-range potential for $r \lesssim 1.5$ fm. For some components of the Paris potential, this short-range phenomenology changes the original theoretic potential considerably, see Fig. 5.

In the final version of the Paris potential, also known as the parametrized Paris potential [14], each component (there is a total of 14 components, 7 for each isospin) is parametrized in terms of 12 local Yukawa functions of multiples of the pion mass. This introduces a very large number of parameters, namely $14 \times 12 = 168$. Not all 168 parameters are free. The various components of the potential are required to vanish at $r = 0$ (implying 22 constraints [14]). One parameter in each component is the πNN coupling constant, which may be taken from other sources (e.g., πN scattering). The 2π-exchange contribution is derived from dispersion theory. The range of this

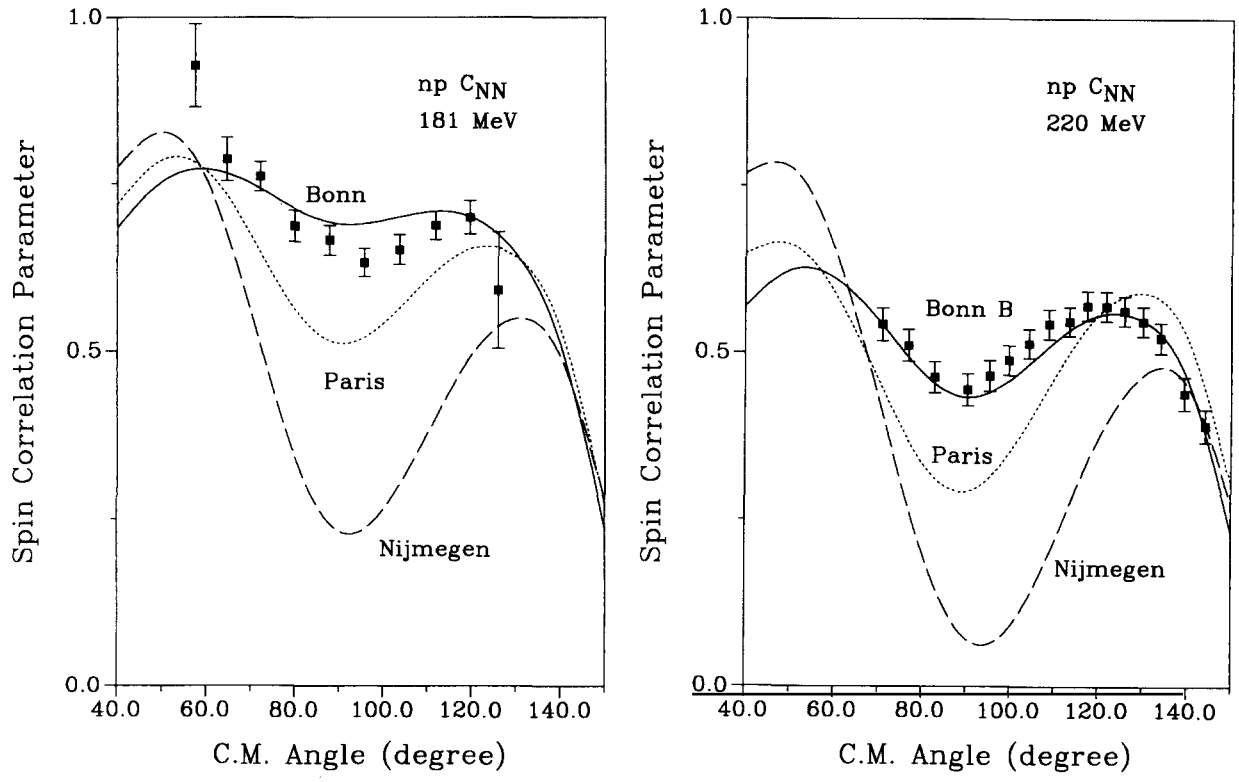

Fig. 3. (a) Neutron–proton spin correlation parameter C_{NN} at 181 MeV. Predictions by the Nijmegen potential [13] (long dashes), the Paris potential [14] (dotted), and the Bonn full model [15] (solid line) are compared with the data (solid squares) from Indiana [18]. The χ^2/datum for the fit of these data is 54.4 for Nijmegen, 3.22 for Paris, and 1.78 for Bonn. The experimental error bars include only systematics and statistics; there is also a scale error of $\pm$ 8%. In the calculations of the χ^2, all three error have been taken into account [25]. (b) Same as (a), but at 220 MeV with the data from TRIUMF [19]. The χ^2/datum for the fit of these data is 121.0 for the Nijmegen, 16.1 for the Paris, and 0.49 for the Bonn *B* potential [6]. In addition to the experimental error shown, there is a scale uncertainty of $\pm$ 5.5%. In the calculation of the χ^2, all errors were taken into account [25].

contribution is typically equivalent to an exchanged mass of 300–800 MeV or, in terms of multiples of the pion mass (m_π), $2m_\pi$–$6m_\pi$. Thus, in parametrized form, this contribution requires 5 parameters per component (implying a total of $5 \times 14 = 70$ parameters) that are fixed by theory and not varied during the best-fit of NN data. In summary, one may assume that about 100 parameters are constrained by the theory underlying the Paris potential; this leaves about 60 free parameters that are used to optimize the fit of the NN data. These parameters mainly determine the short-range part of the Paris potential ($r \lesssim 1.5$ fm), cf. Fig. 5.

Another way to estimate the number of free parameters is to start from the observation that deviations from the original theoretical potential by the best-fit potential occur for $r \lesssim 1.5$ fm (cf. Fig. 5). This range is equivalent to about $6m_\pi$ and more. Thus, the Yukawas with six and more pion masses are affected by the best-fit procedure. Since there are 12 Yukawas, there are seven larger or equal 6; this applies to the 14 components of the potential separately, yielding $7 \times 14 = 98$

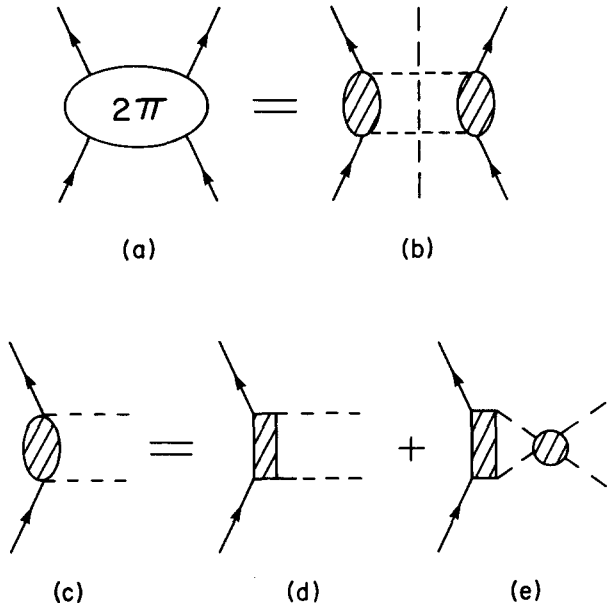

Fig. 4. The 2π-exchange contribution to the NN interaction as viewed by dispersion theory. Solid lines represent nucleons, dashed lines pions.

parameters from which the above mentioned 22 constraints have to be subtracted; the result is 76 fit parameters. Thus, our above estimate of 60 free parameters is on the conservative side.

There are advantages and disadvantages to a large number of fit parameters. The obvious advantage is that with many parameters a good fit of the NN scattering data can easily be obtained; the Paris potential fits the NN data well (see Table 1). However, from a more basic point of view, a large number of phenomenological parameters is discomforting: the theory, underlying the potential, is obscured and, thus, cannot be put to a real test.

To explain the latter point in more detail: for the quantitative description of the low-energy NN data ($E_{\rm lab} \lesssim 300$ MeV), the S-, P-, and D-waves are crucial. A good χ^2 for the fit of the NN data by a potential is due mainly to a good reproduction of the S-, P-, and D-wave phase shifts. These waves are essentially determined by the short-range potential ($r \lesssim 1.5$ fm). Thus, in the Paris potential these lower partial waves are chiefly a product of the phenomenological part of the potential. Consequently, the good fit of the data by the Paris potential has primarily to do with its phenomenological character at short range and not with the underlying meson theory. The theory, the Paris potential is based upon, describes the peripheral partial waves ($L \geq 4$) well (cf. Fig. 7). In fact, the consideration of partial waves with $L \geq 4$ is the real test of the theory underlying the Paris potential, and it passes this test well. However, for the low-energy NN observables, the peripheral waves are of little significance, the bulk is provided by $L \leq 3$.

Thus, by comparing the experimental NN scattering data with the predictions by the Paris potential, meson-theory is not put to a test. This comparison tests the phenomenological potential which is, indeed, consistent with the data. The satisfactory χ^2 of the fit of the data by the Paris potential (cf. Table 1) cannot be used as a proof that meson-theory is correct for the low-energy NN

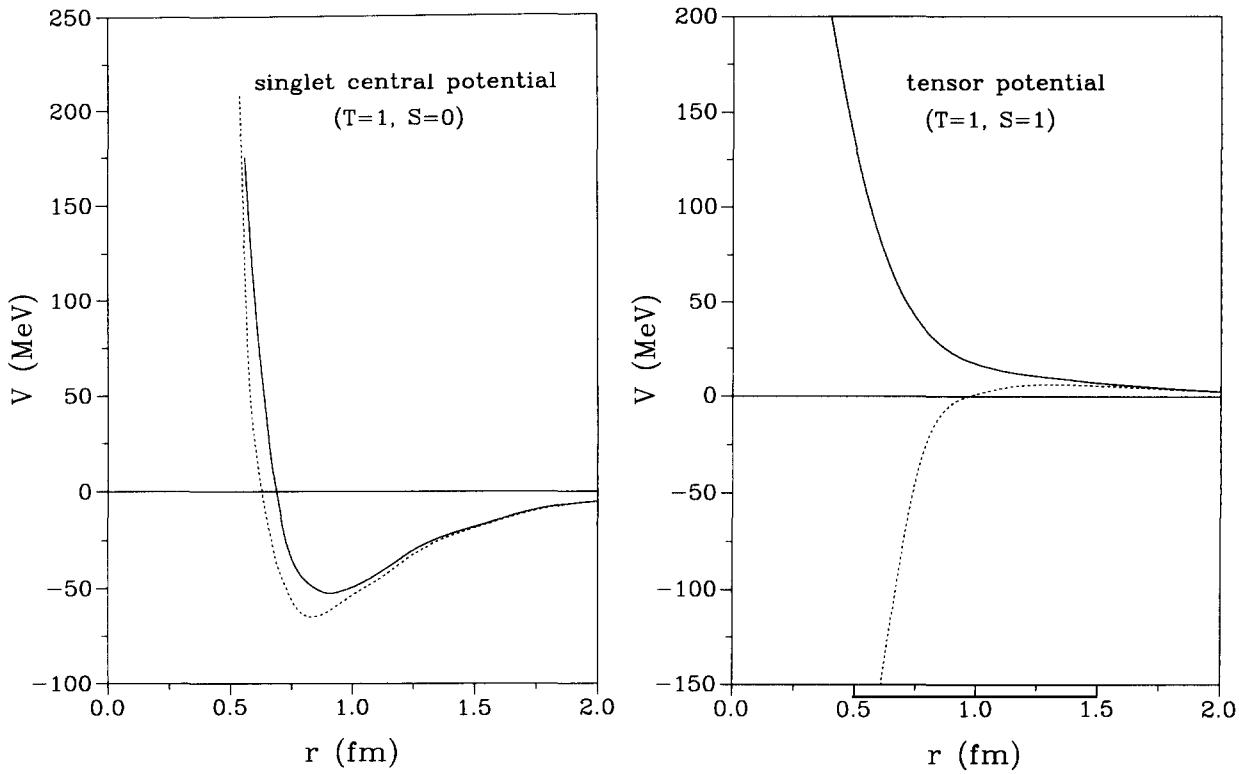

Fig. 5. Two components of the Paris potential: (a) the singlet central potential and (b) the ($T = 1$, $S = 1$) tensor potential. The dotted line represents the result as derived from the underlying theory. The solid line is the parametrized Paris best-fit potential [14].

system. This is unfortunate, since it is this type of information that one would like to draw from a low-energy, meson-theory based potential. In Section 2.4 we will explain how to put meson-theory to a true test.

In microscopic nuclear structure calculations, the off-shell behavior of the NN potential is important (see Section 4 for a detailed discussion). The fit of NN potentials to two-nucleon data fixes them on-shell. The off-shell behavior cannot, by principle, be extracted from two-body data. Theory could determine the off-shell nature of the potential. However, not any theory can do that. Dispersion theory relates observables (equivalent to on-shell T-matrices) to observables; e.g., πN to NN. Thus, dispersion theory cannot, by principle, provide any off-shell information. The Paris potential is based upon dispersion theory; thus, the off-shell behavior of this potential is not determined by the underlying theory. On the other hand, every potential does have an off-shell behavior. When undetermined by theory, then the off-shell behavior is a silent by-product of the parametrization chosen to fit the on-shell T-matrix, with which the potential is identified, by definition. In summary, due to its basis in dispersion theory, the off-shell behavior of the Paris potential is not derived on theoretical grounds. This is a serious drawback when it comes to the question of how to interpret nuclear structure results obtained by applying the Paris potential.

Table 1
Comparison of some meson-theoretic nucleon–nucleon potentials

	Nijmegen [13]	Paris [14]	Bonn full model [15]
# of free parameters	15	≈60	12
Theory includes:			
OBE terms	Yes	Yes	Yes
2π exchange	No	Yes	Yes
$\pi\rho$ diagrams	No	No	Yes
Relativity	No	No	Yes
χ^2/datum for fit of world NN data[a]:			
all pp data	2.06	2.31	1.94
all np data	6.53	4.35	1.88
(np without σ_{tot})	(3.83)	(1.98)	(1.89)
all pp and np	5.12	3.71	1.90

[a] The χ^2/datum are obtained from the computer software SAID of Arndt and Roper (VPI&SU) [25]. The world NN data set in the range 10–300 MeV as of September 1992 is used; it includes 1070 data for pp, 2158 data for np without total cross sections (σ_{tot}), and 2322 data for np with σ_{tot}.

2.3. *The field-theoretic approach to the 2π-exchange*

In a field-theoretic picture, the interaction between mesons and baryons can be described by effective Lagrangians. The NN interaction can then be derived in terms of field-theoretic perturbation theory. The lowest order (that is, the second-order in terms of meson–baryon interactions) are the one-boson-exchange diagrams (Fig. 1), which are easy to calculate.

More difficult (and more numerous) are the irreducible two-meson-exchange (or fourth-order) diagrams. It is reasonable to start with the contributions of longest range. These are the graphs that exchange two pions. A field-theoretic model for this 2π-exchange contribution to the NN interaction is shown in Fig. 6. Naively, one would expect only the two diagrams in the first row of Fig. 6. However, there are two complications that need to be taken into account: meson–nucleon resonances and meson–meson scattering. The lowest πN resonance, the so-called Δ isobar with a mass of 1232 MeV gives rise to the diagrams in the second and third row of Fig. 6. The last two rows include $\pi\pi$ interactions. While two pions in relative P-wave form a resonance (the ρ meson), there is no proper resonance in the $\pi\pi$–S-wave below 900 MeV. However, there are strong correlations in the S-wave at low energies. Durso et al. [22] have shown that these correlations can be described in terms of a broad mass distribution of about 600 ± 260 MeV, which in turn can be approximated by a zero-width scalar-isoscalar boson of mass 550 MeV [15].

At this point, two approaches are available for calculating the 2π-exchange contribution to the NN interaction: dispersion theory (Paris [21]) and field theory (Bonn [15]). Let us now compare the predictions by the two approaches with each other as well as with the data. For this purpose, it is appropriate to look into the peripheral partial waves of NN scattering. In Fig. 7, the curve 'BONN' represents the predictions by the field-theoretic model of Fig. 6; the dotted curve labeled 'P'73' is the original Paris result [21] as obtained from dispersion theory, while the dotted curve

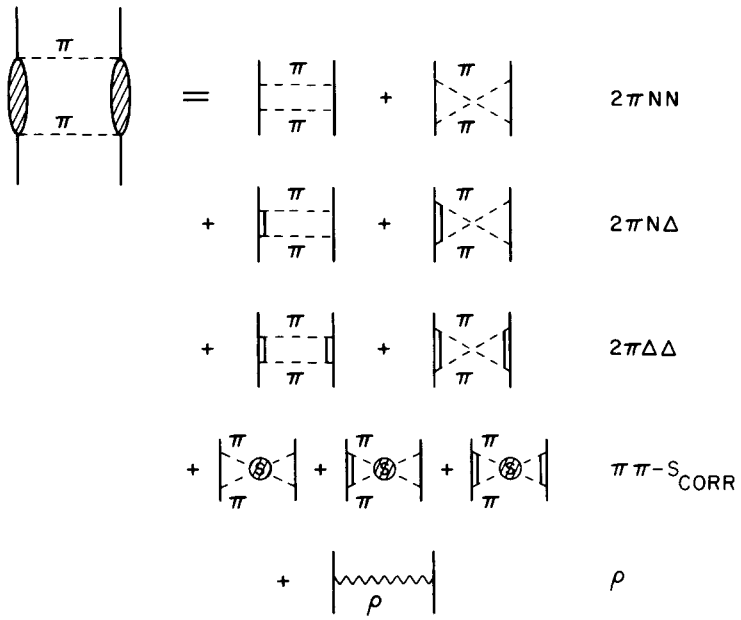

Fig. 6. Field-theoretic model for the 2π-exchange. Solid lines represent nucleons, double lines isobars, and dashed lines pions. The hatched circles are ππ correlations.

'P'80' is the result from the parametrized Paris potential [14] (all curves also contain one-pion and ω-exchange). The agreement between the two theoretical curves and the data is satisfactory. However, there are some substantial deviations (particularly in $^3F_4$) between the theoretical results by the Paris group and their parametrized version. This is puzzling, because we are dealing here with the long- and intermediate-range potential (that is not altered in the parametrization process).

2.4. πρ-contributions and the Bonn potential

As demonstrated in the previous subsection, a model consisting of π + 2π + ω describes the peripheral partial waves quite satisfactory. However, when proceeding to lower partial waves (equivalent to shorter internucleonic distances), this model generates too much attraction. This is true for the dispersion-theoretic result (Paris) as well as the field-theoretic one (Bonn). For *D*-waves, this is seen in Fig. 8 by the curves labelled '2π Paris' and '2π Bonn'. Obviously, further measures have to be taken to arrive at a quantitative model for the NN interaction. It is at this point that the philosophies of the Bonn and Paris group diverge.

The Paris group decided to give up meson theory at this stage and to describe everything that is still missing by phenomenology. Thus, the *S*-, *P*-, and largely also the *D*-waves in the Paris potential are essentially fitted by phenomenology. The difference between the '2π Paris' and the 'Paris' curve in Fig. 8 is the effect of the short-range phenomenological Paris potential chosen such as to fit the empirical phase shifts.

In contrast, the Bonn group continued to consider further irreducible two-meson exchanges. The next set of diagrams to be considered are the exchanges of π and ρ (Fig. 9). Notice that these

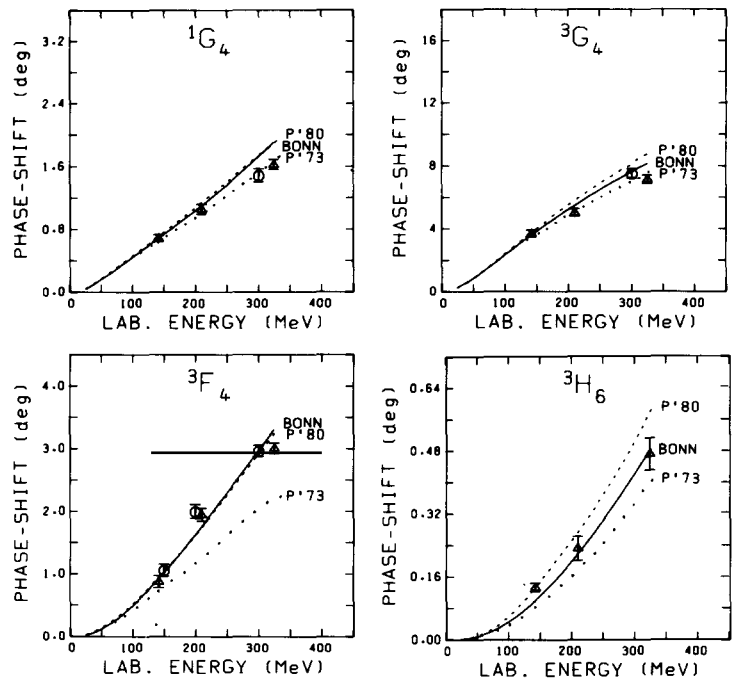

Fig. 7. Phase shifts of some peripheral partial waves as predicted by a field-theoretic model for the 2π exchange (solid line, 'BONN' [15]) and by dispersion theory (dotted line labeled 'P'73' [21]). Both calculations also include OPE and one-ω-exchange. The dotted line labeled 'P'80' is the fit by the parametrized Paris potential [14]. Octagons represent the phase shift analysis by Arndt et al. [23] and triangles the one by Bugg and coworkers [24].

diagrams are analogous to the upper six 2π-exchange diagrams of Fig. 6. The effect of the $\pi\rho$ contributions in D-waves is seen in Fig. 8 by comparing the curve '2π Bonn' with '$2\pi + \pi\rho$ Bonn'. Clearly, these contributions very accurately take care of the discrepancies that were remaining between theory and experiment.

Even more remarkable is the effect of the $\pi\rho$ contributions in S- and P-waves. We show this in Fig. 10 where the dashed line represents the phase shift prediction of the $\pi + 2\pi + \omega$ model while the solid line includes the $\pi\rho$ diagrams.

In Figs. 8 and 10, we have demonstrated clearly that the $\pi\rho$ contributions provide the short-range repulsion which was still missing. It is important to note that the $\pi\rho$ contributions have only one free parameter, namely the cutoff for the $\rho N\Delta$ vertex. The other parameters involved occur also in other parts of the model and were fixed before (like the πNN and ρNN coupling constants and cutoff parameters). *Notice also that the* $\pi N\Delta$ *and* $\rho N\Delta$ *coupling constants are not free parameters, since they are related to the corresponding* NN *coupling constants by* SU(3).

In the light of the $\pi\rho$ results shown, the bad description of some P- and D-waves by some NN potentials (cf. Fig. 2, above) may be simply understood as a lack of the $\pi\rho$ contributions.

In summary, a proper meson-theory for the NN interaction should include the diagrams of irreducible $\pi\rho$ exchange. This contribution has only one free parameter and makes comprehensive short-range phenomenology unnecessary. Thus, meson theory can be truly tested in the low-energy NN system.

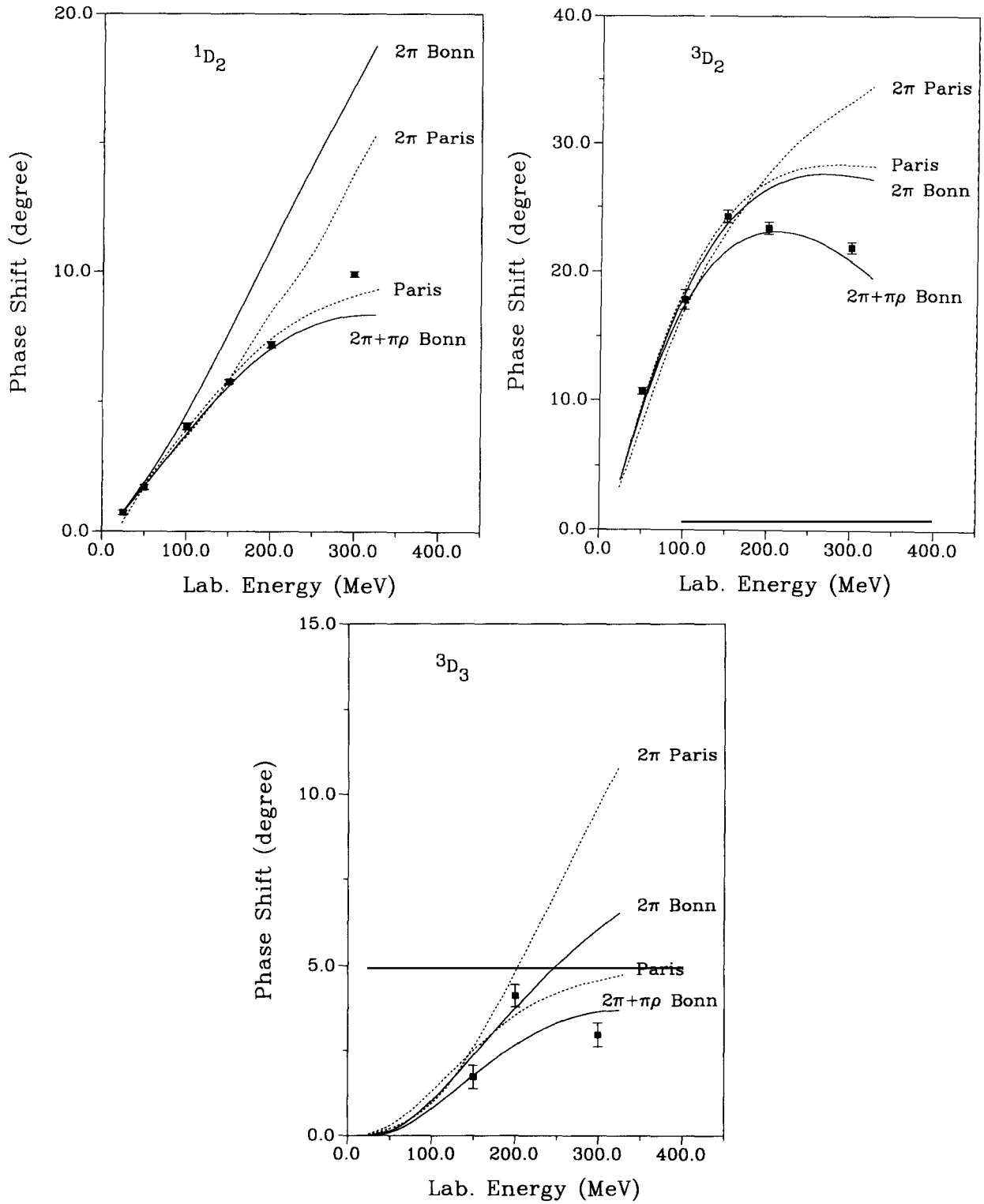

Fig. 8. $\pi\rho$ contributions versus phenomenology in (a) $^1D_2$, (b) $^3D_2$, and (c) $^3D_3$. The curves labeled '2π Paris' and '2π Bonn' represent the predictions by the Paris and Bonn model, respectively, when only the contributions from π, 2π, and ω are taken into account. Adding the phenomenological short-range potential yields the dotted 'Paris' curve (parametrized Paris potential [14]). Adding the $\pi\rho$ contributions (Fig. 9) yields the solid '$2\pi + \pi\rho$ Bonn' curve (Bonn full model [15]).

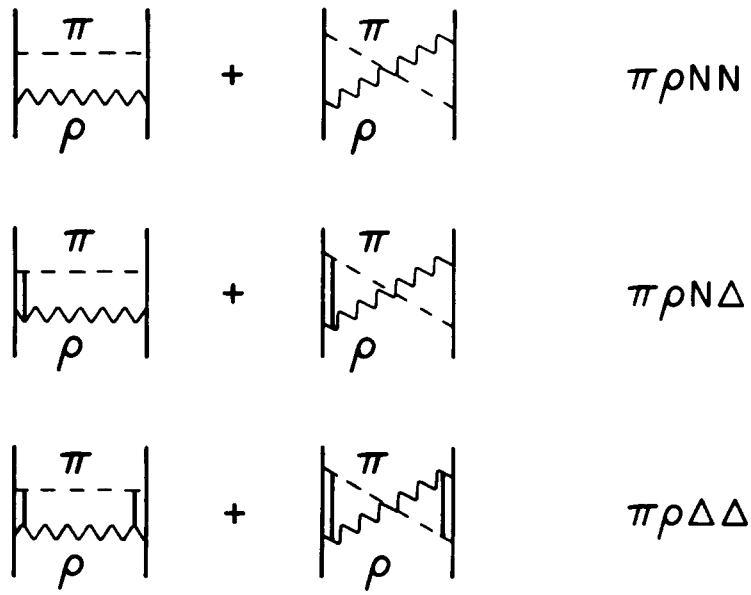

Fig. 9. $\pi\rho$ contributions to the NN interaction.

In the 1970s and 80s, a model for the NN interaction was developed at the University of Bonn. This model consists of single π, ω, and δ exchanges, the 2π model shown in Fig. 6, and the $\pi\rho$ diagrams of Fig. 9, as well as a few more irreducible 3π and 4π diagrams (which are not very important, but indicate convergence of the diagrammatic expansion). This quasi-potential has become known as the 'Bonn full model' [15]. It has 12 parameters which are the coupling constants and cutoff masses of the meson–nucleon vertices involved. With a reasonable choice for these parameters, a very satisfactory description of the NN observables up about 300 MeV is achieved (see Table 1). Since the goal of the Bonn model was to put meson theory at a real test, no attempt was ever made to minimize the χ^2 of the fit of the NN data. Nevertheless, the Bonn full model shows the smallest χ^2 for the fit of the NN data (cf. Table 1).

2.5. *Summary*

In Table 1, we give a summary and an overview of the theoretical input of some meson-theoretic NN models discussed in the previous sections. Moreover, this table also lists the χ^2/datum (as calculated by independent researchers [25]) for the fit of the relevant world NN data, which is 5.12, 3.71, and 1.90 for the Nijmegen [13], Paris [14], and Bonn [15] potential. The compact presentation, typically for a table, makes it easy to grasp one important point: *the more seriously and consistently meson theory is pursued, the better the results.* This table and its trend towards the more comprehensive meson models is the best proof for the validity of meson theory in the low-energy nuclear regime.

While all models considered in Table 1 describe the proton–proton (pp) data well (with χ^2/datum ≈ 2), some models have a problem with the neutron–proton (np) data (with χ^2/datum ≈ 4–6). For

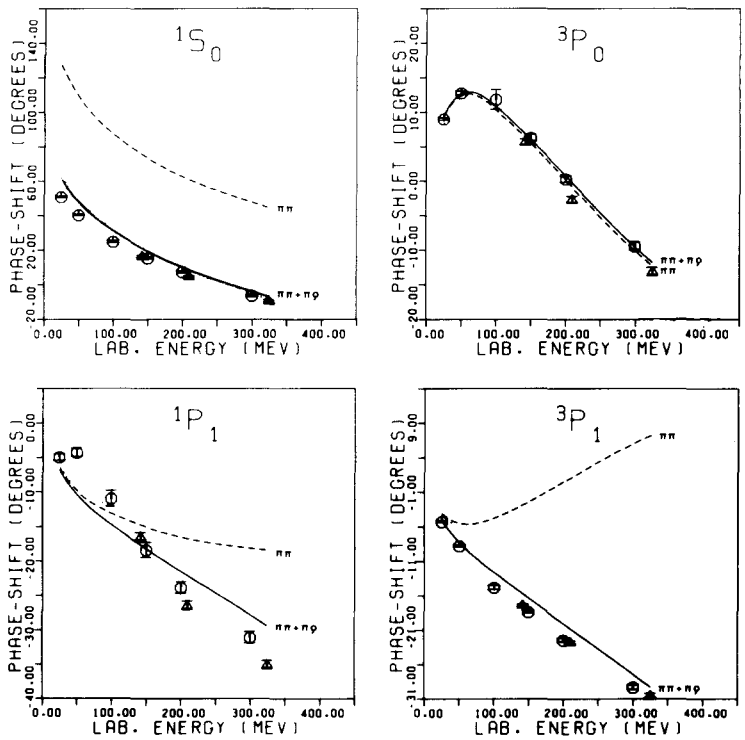

Fig. 10. Effect of the $\pi\rho$ diagrams in some S- and P-waves. The dashed curve is the prediction by the $\pi + 2\pi + \omega$ model. The solid line is obtained when the $\pi\rho$ contributions are added.

the case of the Paris potential (and, in part, for the Nijmegen potential) this is due to a bad reproduction of the np *total cross section* (σ_{tot}) data. When the latter data are ignored, the Paris potential fits np as well as pp (cf. Table 1). The Nijmegen and the Paris potential predict the np total cross sections too large because their $^3D_2$ phase shifts are too large (cf. Fig. 2(b)).

The χ^2 given in Table 1 are calculated for the range 10–300 MeV (in terms of the kinetic energy of the incident nucleon in the laboratory system). This energy interval is very appropriate for reasons that we will explain now.

For very low energies, the effective range expansion applies and the quantitative nature of a potential can be tested by checking how well it reproduces the empirical effective range parameters. We show this in Table 2. It is seen that the Nijmegen and Paris potential reproduce the four S-wave effective range parameters very badly in terms of the χ^2/datum, which is 95 and 169, respectively. In the case of the Paris potential, this is entirely due to a wrong prediction for a_{pp}^C, which is off by 26 standard deviations; the other three parameters are described well. For reasons of fairness, one should note that the empirical value for a_{pp}^C has a very small error (namely, 0.0026 fm). This may blow up small deviations by theory from experiment in a misleading way. In absolute terms, the Paris a_{pp}^C is wrong by only 0.07 fm. This is negligible with regard to any nuclear structure application.

The Nijmegen potential is off by about 10 standard deviations for every parameter listed in Table 2. The large discrepancy between the triplet parameters as predicted by the Nijmegen

Table 2
Low-energy S-wave scattering parameters as predicted by some meson-theoretic NN potentials. In the last row, the χ^2/datum is given for the fit of the 4 empirical data given in the last column

	Nijmegen [13]	Paris [14]	Bonn full model [15]	Empirical
Singlet:				
a_{pp}^C (fm)	−7.797	−7.887[a]	−7.8197[b]	−7.8196(26)[c]
r_{pp}^C (fm)	2.697	2.805[a]	2.7854[b]	2.790(14)[c]
Triplet:				
a (fm)	5.468	5.427	5.427	5.424(4)[d]
r (fm)	1.818	1.766	1.755	1.759(5)[d]
χ^2/datum	95.0	168.9	0.33	—

[a] The predictions by the Paris potential for a_{pp}^C and r_{pp}^C given in this table were obtained in independent calculations by Piepke [26] and the Nijmegen group [27]; they differ from Ref. [14].
[b] See appendix.
[c] From Ref. [27].
[d] From Ref. [28].

potential and the empirical ones is a reflection of the fact that the Nijmegen $^3S_1$ phase shifts are in general too low and too steep; e.g., at 210 MeV, the Nijmegen potential predicts 14.91° for the $^3S_1$ phase shift which is 12 standard deviations below the value from the phase shift analysis (which is $19.0 \pm 0.33°$ [25]).

It is unreasonable to consider energies higher than 300 MeV to test real NN potential models. Around 285 MeV pion production starts. Thus, strictly speaking, a real NN potential is inadequate above that energy. It may be all right to stretch this limit by a few MeV up to 300 MeV (for practical reasons, since phase shift analyses often state their results in steps of 100 MeV), but not beyond that. Also it is quite consistent and by no means accidental that the χ^2 for the fit of, particularly, the np data becomes very bad above 300 MeV for all potential models we are aware of. For example, for the 567 neutron–proton data in the energy range 300–350 MeV the χ^2/datum is 18.0, 7.2, and 6.4 for the Nijmegen, Paris, and Bonn potential, respectively. These χ^2 are larger by about a factor of three as compared to the ones for the data below 300 MeV (cf. Table 1).

In the literature, it is sometimes stressed that some real potentials do particularly well for energies above 300 MeV. It is hard to understand how it can be of any significance when a real potential is doing well in an energy range where, by principle, the real potential concept is inadequate.

In Fig. 11, we give an overview of the fit of phase shifts by some modern meson-theoretic potentials. The solid line represents the prediction by the Bonn full model [15] while the dashed line is the Paris [14] prediction. The Bonn full model is an energy-dependent potential. This energy-dependence is inconvenient in nuclear structure applications. Therefore, a representation of the model in terms of relativistic, energy-independent Feynman amplitudes has been developed, using the relativistic, three-dimensional Blankenbecler–Sugar method [30]. This representation has become known as the 'Bonn B potential' [6][5]. The dotted line in Fig. 11 shows the phase-shift

[5] For more details, see [6, Section 4, Appendix A and Table A.1].

predictions by the Bonn B potential, which are very similar to the ones by the Bonn full model. For the Bonn B potential, the χ^2/datum is 2.1 for the 2158 np data without σ_{tot} and 2.3 for the 2322 np data including σ_{tot} in the energy range 10–300 MeV (cf. Table 1). These numbers reflect well the fact that the Bonn B potential describes the NN scattering data in close agreement with experiment as well as with the predictions by the Bonn full model. Moreover, since Bonn B, like full Bonn, uses the full, relativistic Feyman amplitudes, it is a nonlocal potential. Therefore, it has a rather different off-shell behavior than local potentials and, thus, leads to different (but interesting) results in nuclear structure (see Section 4).

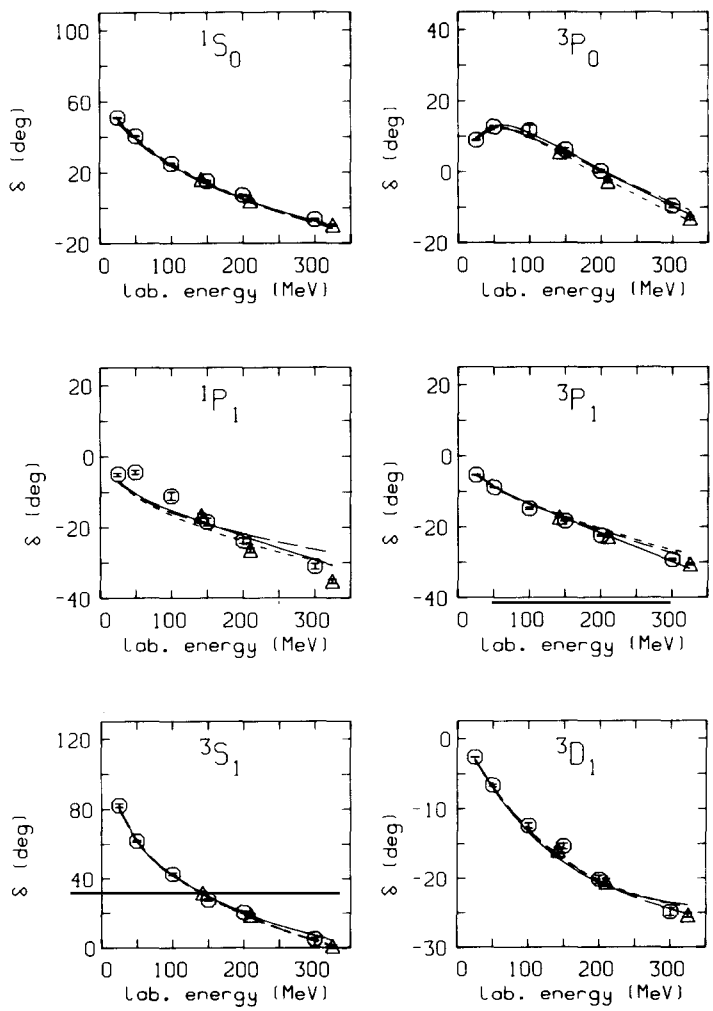

Fig. 11. Overview of the fit of phase shifts by some current models for the NN interaction. Predictions are shown for the Bonn full model [15] (solid line), the Paris potential [14] (dashed), and the Bonn B potential [6] (dotted). Octagons represent the phase shift analysis by Arndt et al. [23], triangles the one by the Dubois et al. [24], and the solid dot is from the recent analysis by Bugg [29].

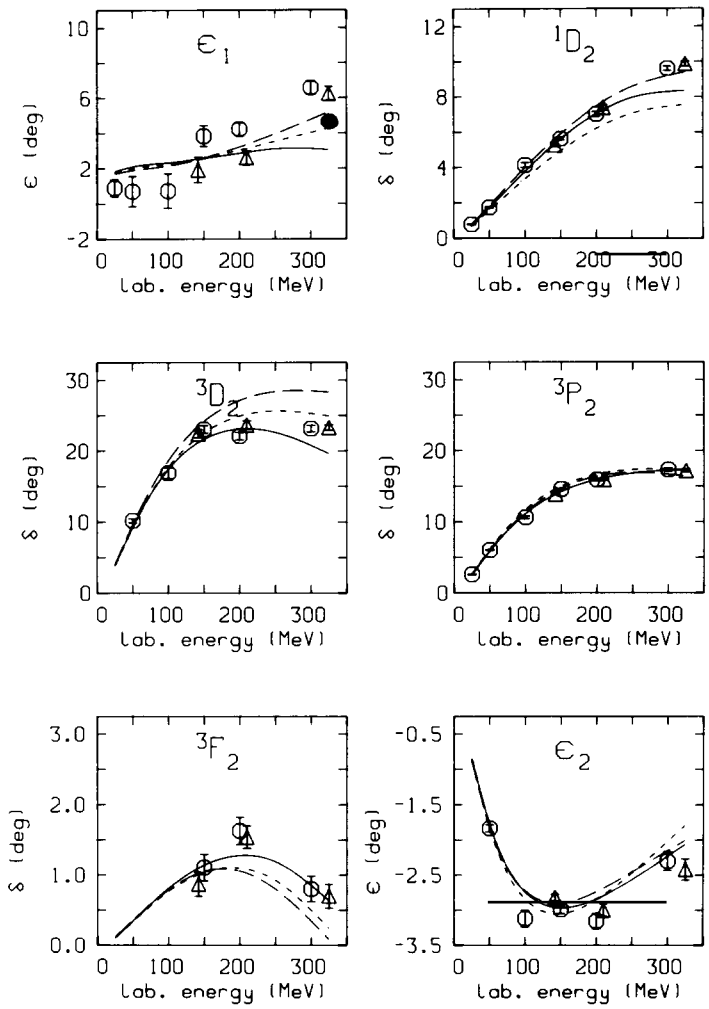

Fig. 11. (continued)

3. Polemics

Recently, there has been some debate about the 'quality' of different NN potentials. In particular, the χ^2 of the fit of the experimental NN data by a potential has sometimes become an issue. Unfortunately, this debate has not always been conducted in a strictly scientific manner. Therefore, we like to take this opportunity for a few comments, in the hope that this may help to lead the discussion back to more scientific grounds.

(1) *The χ^2 is not a magic number.*

Its relevance with regard to the 'quality' of a potential is limited. Consider, for example, a model based on little theory, but with many parameters; this model will easily fit the data well and produce a very low χ^2 (e.g., χ^2/datum ≈ 1). But we will not learn much basic physics from this. On

the other hand, think of a model with a solid theoretic basis and (therefore) very few parameters (with each parameter having a physical meaning); here, the comparison with the experimental data may teach us some real physics. In such a case, a χ^2/datum of 2 or 3 may be excellent.

Thus, the χ^2 represents only one aspect among several others that need to be considered simultaneously when judging the quality of a NN potential. Other aspects of equal importance are the theoretical basis of a potential model (see the previous section) and (closely related) its off-shell behavior (that can, of course, not be tested by calculating the χ^2 with regard to the on-shell NN data). This latter aspect is important, particularly, for the application of a NN potential to nuclear structure. In fact, in Section 4 we will give an example, in which the variation of the χ^2/datum between 1 and 6 affects nuclear structure result only in a negligible way, while off-shell differences are of substantial influence.

Notice also, that the χ^2 sometimes blows up small differences between theory and experiment in a misleading way. This is so, in particular, when the experimental error is very small (a good example for this are the pp data below 3 MeV, see discussion below). In such cases, the χ^2 is more a reflection of the experimental precision than of the quality of the theory.

In summary, the χ^2 must be taken with a grain of salt; overestimating the importance of the χ^2 may miss the physics.

(2) *If one considers the* χ^2*, it is insufficient to consider it for the* pp *data only.*

In some recent work on χ^2, persistently only pp data are considered [31, 32]. Since some potentials fit the pp data much better than np (cf. Table 1), it may be tempting to do so (for reasons that, however, have little to do with physics). pp states exist only for $T = 1$ and, thus, a comparison with the pp data tests only the $T = 1$ potential. Confrontation with np data tests both $T = 1$ and $T = 0$ and, thus, is a much more comprehensive test of a potential. In fact, the problems of some potentials shown in Figs. 2 and 3 are due to $T = 0$ states and, thus, are missed when only pp is considered. Moreover, in nuclear structure calculations, typically both the $T = 0$ and the $T = 1$ potential is needed. In nuclear structure, the $T = 0$ states are in general as important as the $T = 1$ states (in fact, one may well argue that the $T = 0$ states are even more crucial since the very important $^3S_1$ states is $T = 0$).

(3) *If one calculates a* χ^2*, one should do it by all means properly.*

The most important rule here is: a pp *potential must only be confronted with* pp *data, while a* np *potential must only be confronted with* np *data.* Though this rule is obvious, it has sometimes been violated even by experts in the field. Let us briefly explain why this rule is so important. At low energies, NN scattering takes place mainly in S-wave. There is well-known charge-dependence in the $^1S_0$ state and, moreover, the electromagnetic effects are very large in low energy pp scattering. Thus, np and pp differ here substantially. Moreover, there exist very accurate pp cross section data at low energies. Consequently, if (improperly) a np potential is applied to pp scattering, a very large χ^2 is obtained. However, this χ^2 simply reflects the fact that charge-dependence and Coulomb distorsion are important and the pp data carry a small error at low energy.

To give an example: when the np versions of the Argonne [8] and Bonn [15] potentials are (improperly) confronted with the pp data, a χ^2/datum of 824 and 641, respectively, is obtained [31]. However, if (properly) the pp version of the Bonn potential (see appendix) is confronted with the pp data, a χ^2/datum of 1.9 is obtained (cf. Table 1).

Notice also that the change in the potential, that brings about this enormous change in the χ^2, is minimal. The main effect comes from the $^1S_0$. A np potential is fit to the np value for the singlet

scattering length. Now, if one wants to construct a pp potential from this, one has to do essentially only two things: the Coulomb force has to be included and the singlet scattering length has to be readjusted to its pp value. Since the scattering length of an almost bound state is a super-sensitive quantity, this is achieved by a very small change of one of the fit parameters; for example, a change of the σ coupling constant by as little as 1%. This is all that needs to be done; this changes the χ^2/datum by several 100.

The difference in the $^1S_0$ phase shift between pp and np is as small as the difference between the solid and the dashed curve in the $^1S_0$ box of Fig. 11 (which on the scale of the figure can hardly be seen). When applied to nuclear matter, this difference makes a change in the energy per nucleon of about 0.5 MeV (of about 16 MeV total binding energy per nucleon). Thus, we are dealing here with a very subtle difference, which by accident makes a difference in the χ^2/datum of 1.9 versus 600. It shows in a clear way how misleading χ^2 can be if the reader is not familiar with the field.

In any case, if one wants to test a np potential, why not compare it with the np data? That's the most obvious thing to do; it's straightforward, and nothing can be done wrong. Moreover, this tests the $T = 0$ and $T = 1$ potential at once; thus, it is a comprehensive and complete test of the quantitative nature of a potential. There is no need to bring by all means the pp data into play [except that for some potentials the pp χ^2 is much better than the np one (cf. Table 1)].

Some potentials developed in the 1980's [8, 15, 6] are fit to the np data, while older models, e.g. Refs. [5, 13], were in general fit to pp. The preference for fitting np rather than pp in recent years has good reasons that we will explain now. Nowadays, phase shift analyses, see e.g. Refs. [23, 16], are conducted in the following manner. First, the pp data are analysed to determine the pp phase shifts. After this, the np analysis is started. However, this np analysis is not performed independently, i.e. it is not based upon the np data only. The reason for this is that there are twice as many partial waves for np than for pp. Therefore, a np phase shift analysis based upon the np data only would have larger uncertainties. Thus, for the $T = 1$ np phase shifts (except $^1S_0$), the pp analysis is used, after two corrections have been applied. The Coulomb effect is removed and, in some cases, a simple assumption about charge-dependence is applied (e.g. the charge-dependence of the one-pion-exchange due to pion-mass difference). Again, this is done for $L > 0$; for $^1S_0$ an independent np analysis is performed (confirming the well-established charge-dependence in that state as seen most clearly in the well-known scattering length differences). The result of the entire phase-shift analysis is then stated in terms of np phase shifts [23, 16].

Now, from the way pp and np phase shift analyses are conducted, it is clear that a potential that fits the np phase shifts well, will automatically fit the pp phase shifts well, *after the small but important corrections for Coulomb and charge-dependence have been applied* (similarly to what is done in the phase shift analysis). A good example for this is the Bonn potential that has originally been fit to np [15] and has a χ^2/datum of 1.9 for the world np data (cf. Table 1). Now, when the Coulomb force is included and the $^1S_0$ scattering length is adjusted to its pp value, then the world pp data are reproduced with a χ^2/datum of also 1.9 (instead of 641 [31], which is a meaningless number).

In a more recent series of χ^2 calculations [32], the Argonne and the Bonn np potentials are again (improperly) confronted with the pp data. For the pp data in the energy range 2–350 MeV a χ^2/datum of 7.1 and 13, respectively, is obtained (while for the range 0–350 MeV, the corresponding numbers are 824 and 641, as mentioned above). However, to cut out the range 0–2 MeV is

insufficient. Charge dependence is important up to about 100 MeV. Thus, these new χ^2 calculations [32] are again meaningless. Moreover, in Ref. [32] the 'Bonn 87' model [15] is identified with a local r-space OBEP. This is very incorrect and misleading. In Ref. [15] the Bonn full model is presented with which, therefore, the Bonn model of 1987 is to be identified. Clearly, a Physics Reports article published in 1987 does not serve the purpose to present a simplistic model appropriate for the 1960s. Since Ref. [15] is a review article, it also contains some discussion of other (simpler) models. In particular, comparison is made with the local r-space concept (denoted by OBEPR in Ref. [15]) to point out the deficiencies of such simple models in fitting certain phase shifts (similarly to what we explain Section 2.1 of this contribution) and to discuss to which extend such models may still be useful in some nuclear structure applications. But clearly, OBEPR is not 'the Bonn model' and the χ^2 of OBEPR is of no interest.

4. NN potentials and nuclear structure

One of the major topics of this workshop are nuclear structure calculations based upon the bare NN interaction. This program was started some 25 years ago by Kuo and Brown [1].

For these miscroscopic nuclear structure calculations, a crucial question is: what role do the differences between different NN potentials play? We will try to answer this question in this section. It is appropriate to subdivide the discussion into on-shell and off-shell aspects.

4.1. On-shell properties and nuclear structure

By definition, we mean by 'on-shell properties of nuclear potentials' their predictions for the deuteron and low-energy two-nucleon scattering observables ($\lesssim$300 MeV lab. energy).

To demonstrate the influence of on-shell differences on nuclear structure results, one needs to find a case, where two potentials are essentially identical off-shell (including the strength of the tensor force, see discussion below), but differ on-shell. It is not easy to isolate such a case, since, in general, different potentials show differences on- and off-shell.

Recently, the Nijmegen group has constructed a revised version [33] of their original potential [13]. To improve the reproduction of the NN data, the new Nijmegen potential fits the phase shifts of each NN partial wave separately (allowing for a different set of fit parameters for each partial wave). This is similar to the approach that Reid took some 25 years ago [5] and, thus, this new potential is sometimes referred to as the Nijmegen 'Reid-like' potential [33]. In this approach, it is, of course, easy to obtain a perfect fit of the NN scattering data. Since both Nijmegen potentials are defined in terms of the same mathematical expressions, they have the same off-shell properties; in particular, they yield almost the same D-state probability for the deuteron, implying equal tensor force strength. Thus, these two Nijmegen potentials represent an excellent example for two potentials that are the same off-shell. Now, on-shell these two potentials differ, since the more recent one fits the NN data below 300 MeV much better than the older one. This is seen most clearly in the χ^2/datum for the fit of the world np data (including σ_{tot}) which is improved from 6.5 for the old Nijmegen potential to 1.0 for the new potential. Notice that this difference in the χ^2 is substantial; probably the largest on-shell difference that exists for any two realistic NN potentials.

The question now is: how do these large on-shell differences affect nuclear structure results?

To answer this question, it is best to consider a nuclear structure quantity for which an exact calculation can be performed. We choose the binding energy of the triton. Rigorous Faddeev calculations, which solve the three-body problem exactly, are feasible and have actually been performed for the two Nijmegen potentials under discussion. The results are summarized in Table 3: we see that the old Nijmegen potential [13] with a χ^2/datum of 6.5 predicts 7.63 MeV [34] for the triton binding, while the new potential with a χ^2/datum of 1.0 yields 7.62 MeV [35]. Thus, in spite of the seemingly very large differences on-shell in terms of the χ^2, the difference in the nuclear structure quantity under consideration is negligibly small.

On the other hand, consider two potentials that have an almost identical χ^2 for the world np data (implying that they are essentially identical on-shell). Accidentally, this is true for the Paris [14] and the Bonn *B* [6] potential, which both have a χ^2/datum of about 2 (cf. Table 3). The triton binding energy predictions derived from these two potentials are 7.46 MeV for the Paris potential and 8.13 MeV for Bonn *B*. This appears like a contradiction to the previous results. With the χ^2 so close, naively, one would have expected identical triton binding energy predictions. Obviously there is another factor, even more important than the χ^2: this factor is the off-shell behavior of a potential (particularly, the off-shell tensor force strength, that can vary substantially for different realistic potentials). A simple measure for this strength is the D-state probability of the deuteron, P_D, with a smaller P_D implying a weaker (off-shell) tensor force. For this reason, we are also giving in Table 3 the P_D for each of the potentials under consideration. The real reason for the differences in the predictions by Paris and Bonn *B* is the difference in the P_D with Paris predicting 5.8% and Bonn *B* 5.0% (cf. Table 3).

Summarizing: on-shell differences between potentials are seen in differences in the χ^2 for the fit of the NN data; off-shell differences are seen in differences in P_D. As Table 3 reveals, off-shell differences are much more important than on-shell differences for the triton binding energy.[6]

A similar consideration can be done for nuclear matter. This is summarized in Table 4. In this example, we are more specific as far as the χ^2 is concerned. We have choosen a particular set of NN

Table 3
Correlations between two-nucleon and three-nucleon properties as predicted by different NN potentials. The χ^2/datum is related to the on-shell properties of a potential, while P_D depends essentially on the off-shell behavior

	Nijmegen [13]	Nijm.–Reid [33]	Bonn B [6]	Paris [14]
Two-nucleon data:				
χ/datum[a]	3.8	1.0	2.1	2.0
P_D (%)[b]	5.4	5.6	5.0	5.8
Triton binding (MeV):	7.63	7.62	8.13	7.46

[a] for the fit of the world np data (without σ_{tot}) in the range 10–300 MeV (cf. Table 1).
[b] D-state probability of the deuteron.

[6] Here and in the following, it is understood that we consider only realistic potentials that yield a reasonable description of the empirical NN data. Arbitrary on-shell variations may, of course, have large effects on nuclear structure predictions.

data, namely the np analysing power (A_y) data at 25 MeV, which have been measured with great accuracy [36]. This experimental data set tests, in particular, the triplet P-waves. Note, that differences between modern potentials occur mainly in these P-waves (besides the ones in D-waves shown in Fig. 2). We consider now two potentials which fit these data perfectly, namely Paris and Bonn B (χ^2/datum around 1 in both cases) and another potential with the rather poor χ^2/datum of 3.3 (denoted by 'Potential B'''). These three potentials are applied to nuclear matter in a standard Brueckner calculation. It turns out (see Table 4) that the large χ^2 difference between Bonn B and Potential B' makes only a difference of 0.3 MeV in the nuclear matter energy. On the other hand, the nuclear matter predictions by the other two potentials (with identical and perfect fit) differ by as much as 1.4 MeV. As in the case of the triton, the difference in P_D is the reason. [Notice that this difference shows up in the $^3S_1$ contribution (cf. Table 4).]

Again, the off-shell behavior turns out to be of great relevance. We will now discuss these off-shell aspects in more detail.

4.2. *Off-shell effects*

For a given NN potential V, the T-matrix for free-space two-nucleon scattering is obtained from the Lippmann–Schwinger equation, which reads in the center-of-mass system

$$T(\boldsymbol{q}', \boldsymbol{q}) = V(\boldsymbol{q}', \boldsymbol{q}) - \int \mathrm{d}^3k\, V(\boldsymbol{q}', \boldsymbol{k}) \frac{M}{k^2 - q^2 - \mathrm{i}\varepsilon} T(\boldsymbol{k}, \boldsymbol{q}) \tag{1}$$

and in partial-wave decomposition

$$T^{JST}_{L'L}(q', q) = V^{JST}_{L'L}(q', q) - \sum_{L''} \int_0^\infty k^2\, \mathrm{d}k\, V^{JST}_{L'L''}(q', k) \frac{M}{k^2 - q^2 - \mathrm{i}\varepsilon} T^{JST}_{L''L}(k, q) \tag{2}$$

where J, S, T, and L denote the total angular momentum, spin, isospin, and orbital angular momentum, respectively, of the two nucleons; and M is the mass of the free nucleon. $\boldsymbol{q}$, $\boldsymbol{k}$, and $\boldsymbol{q}'$ are the initial, intermediate, and final relative three-momenta, respectively ($q' \equiv |\boldsymbol{q}'|$, $k \equiv |\boldsymbol{k}|$, $q \equiv |\boldsymbol{q}|$).

Notice that the integration over the intermediate momenta k in Eqs. (1) and (2) extends from zero to infinity. For intermediate states with $k \neq q$, energy is not conserved and the nucleons are off their energy shell ('off-shell'). The off-shell part of the potential (and the T-matrix) is involved. Thus, in the integral term in Eqs. (1) and (2), the potential (and the T-matrix) contributes essentially off-shell.

However, the off-shell potential does not really play any role in free-space NN scattering. The reason for this is simply the procedure by which NN potentials are constructed. The parameters of NN potentials are adjusted such that the resulting on-shell T-matrix fits the empirical NN data. For our later discussion, it is important to understand this point. Let us consider a case in which the off-shell contributions are particularly large, namely the on-shell T-matrix in the $^3S_1$ state:

$$\begin{aligned} T^{110}_{00}(q, q) = {} & V^{110}_{00}(q, q) - \int_0^\infty k^2\, \mathrm{d}k\, V^{110}_{00}(q, k) \frac{M}{k^2 - q^2 - \mathrm{i}\varepsilon} T^{110}_{00}(k, q) \\ & - \int_0^\infty k^2\, \mathrm{d}k\, V^{110}_{02}(q, k) \frac{M}{k^2 - q^2 - \mathrm{i}\varepsilon} T^{110}_{20}(k, q)\,, \end{aligned} \tag{3}$$

Table 4
Correlations between two-nucleon and nuclear matter properties for different potentials. Nuclear matter with a Fermi momentum of $k_F = 1.35\,\mathrm{fm}^{-1}$ is considered

	Bonn B [6]	Potential B'	Paris [14]
Two-nucleon data:			
χ^2/datum[a]	1.0	3.3	1.1
P_D (%)[b]	5.0	5.0	5.8
Nuclear matter energy (MeV):			
$^3S_1$ contribution	−18.8	−18.8	−17.1
Total	−12.1	−11.8	−10.7
Difference to Bonn B	—	0.3	1.4

[a] for the fit of the np analysing power data at 25 MeV (16 data points) [36].
[b] D-state probability of the deuteron.

Up to second-order in V, this is

$$T_{00}^{110}(q,q) \approx V_{00}^{110}(q,q) - \int_0^\infty k^2\,\mathrm{d}k\,V_{00}^{110}(q,k)\,\frac{M}{k^2-q^2-\mathrm{i}\varepsilon}\,V_{00}^{110}(k,q)$$
$$- \int_0^\infty k^2\,\mathrm{d}k\,V_{02}^{110}(q,k)\,\frac{M}{k^2-q^2-\mathrm{i}\varepsilon}\,V_{20}^{110}(k,q)\,, \tag{4}$$

$$\approx V_{00}^{110}(q,q) - \int_0^\infty k^2\,\mathrm{d}k\,V_{02}^{110}(q,k)\,\frac{M}{k^2-q^2-\mathrm{i}\varepsilon}\,V_{20}^{110}(k,q)\,, \tag{5}$$

where in the last equation, we also neglected the second-order in V_{00}^{110} which is, in general, much smaller than the second-order in V_{02}^{110}. Or, without partial-wave decomposition

$$T(\boldsymbol{q},\boldsymbol{q}) \approx V_C(\boldsymbol{q},\boldsymbol{q}) - \int \mathrm{d}^3k\,V_T(\boldsymbol{q},\boldsymbol{k})\,\frac{M}{k^2-q^2-\mathrm{i}\varepsilon}\,V_T(\boldsymbol{k},\boldsymbol{q})\,, \tag{6}$$

where V_C denotes the central force and V_T the tensor force. The tensor force makes possible transitions between states that are not diagonal in L.

The on-shell T-matrix is related to the observables that are measured in experiment. Thus, potentials which fit the same NN scattering data produce the same on-shell T-matrices. However, this does not imply that the potentials are the same. As seen in Eqs. (1) and (2), the T-matrix is the sum of two terms, the Born term and an integral term. When this sum is the same, the individual terms may still be quite different.

Let us consider an example. The T-matrix in the $^3S_1$ state is attractive below 300 MeV lab. energy. If a potential has a strong (weak) tensor force, then the integral term in Eq. (5) is large (small), and the negative Born term will be small (large) to yield the correct on-shell T-matrix element.

In Fig. 12 we show the $^3S_1$–$^3D_1$ potential matrix element, $V_{02}^{110}(q,k)$, for the Paris and the Bonn B potential. The momentum q is held fixed at 153 MeV which is equivalent to a lab. energy of

50 MeV ($E_{lab} = 2q^2/M$). The abscissa, k, is the variable over which the integration in Eq. (5) is performed. It is seen that, particularly for large off-shell momenta, the Bonn B potential is smaller than the Paris potential. However, notice also that at the on-shell point ($q = k$, solid dot in Fig. 12) both potentials are identical (both potentials predict the same ε_1 parameter). Thus, the Bonn B potential has a weaker *off-shell* tensor force than the Paris potential. Since the Bonn B and the Paris potential predict almost identical phase shifts[7], the Born term (central force) in the $^3S_1$ state will be more attractive for the Bonn B potential than for the Paris potential.

In summary, Fig. 12 demonstrates in a clear way how large off-shell differences can be between two realistic potentials that produce identical phase parameters (identical on-shell T-matrices).

A neat measure of the strength of the nuclear tensor force is the D-state probability of the deuteron, P_D. This quantity is defined as

$$P_D = \int_0^\infty q^2 \, dq \, \psi_2^2(q) \,, \tag{7}$$

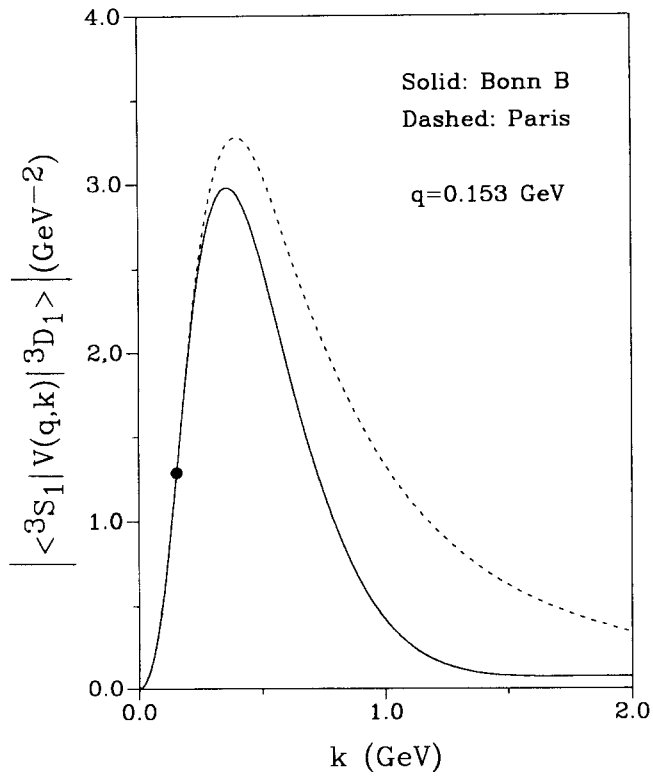

Fig. 12. Magnitude of the half off-shell potential $\langle {}^3S_1|V(q,k)|{}^3D_1\rangle \cdot q$ is held fixed at 153 MeV. The solid curve is the Bonn B potential [6] and the dashed curve the Paris potential [14]. The solid dot denotes the on-shell point ($k = q$).

[7] For the $^3S_1$ phase shift at 50 MeV, Paris predicts 62.3° and Bonn-B 62.2°.

where ψ_2 denotes the deuteron D-wave in momentum space. The deuteron waves are obtained from a system of coupled integral equations

$$\psi_L(q) = -\frac{1}{B_d + q^2/M} \sum_{L'} \int_0^\infty k^2 \, dk \, V_{LL'}^{110}(q, k) \psi_{L'}(k) \tag{8}$$

where B_d denotes the binding energy of the deuteron. Approximately, we can write for the D-wave

$$\psi_2(q) \approx -\frac{1}{B_d + q^2/M} \int_0^\infty k^2 \, dk \, V_{20}^{110}(q, k) \psi_0(k) \tag{9}$$

where ψ_0 denotes the deuteron S-wave. Notice that the off-shell potential shown in Fig. 12 is integrated over here. This explains why the D-state probability for Bonn B is smaller than for Paris, in spite of both potentials having the same on-shell properties.

In the Brueckner approach to the nuclear many-body problem, a G-matrix is calculated which is the solution of the equation

$$G(\boldsymbol{q}', \boldsymbol{q}) = V(\boldsymbol{q}', \boldsymbol{q}) - \int d^3k \, V(\boldsymbol{q}', \boldsymbol{k}) \frac{M^* Q}{k^2 - q^2} G(\boldsymbol{k}, \boldsymbol{q}) \tag{10}$$

The similarity to the Lippmann–Schwinger equation, eq. (1), is obvious. There are differences in two points: the Pauli projector Q and the energy denominator. (For simplicity, we have assumed the so-called continuous choice for the single particle energies in nuclear matter, i.e. the energy of a nucleon is represented by $\varepsilon(p) = p^2/(2M^*) - U_0$ for $p \leq k_F$ as well as $p > k_F$, where M^* is the effective mass and U_0 a constant.) The Pauli projector prevents scattering into occupied states and, thus, cuts out the low momenta in the k integration. The difference introduced by the Pauli projector is known as the Pauli effect, the energy denominator gives rise to the so-called dispersive effect. When using the continuous choice, the dispersive effect is given simply by the replacement of M by M^* ($\approx 2/3M$ at nuclear matter density) in the numerator of the integral term, which simply leads to a reduction of this attractive term by a factor M^*/M. Both effects go into the same direction, namely they quench the integral term. Since the integral term is negative, these effects are repulsive.

From our previous discussion, we know already that a potential with a weak tensor force (small P_D) produces a smaller integral term than a strong tensor-force potential. Thus, the G-matrix resulting from a strong-tensor force potential will be subject to a larger quenching; thus, the G-matrix will be less attractive than the one produced by a weak-tensor force potential. This explains why NN interactions with a weaker tensor force yield more attractive results when applied to nuclear few- and many-body systems.

In the case of the three-nucleon system, the formalism is different, but the mechnisms at work are very similar. A two-nucleon T-matrix is used as input for the Faddeev equations. The energy parameter of this T-matrix runs from -8.5 MeV to $-\infty$, causing a large dispersive effect (there is no Pauli effect).

We show now three examples which demonstrate clearly these differences in predictions for nuclear energies by weak tensor-force potentials *versus* strong tensor-force potentials. As examples we choose the binding energy of the triton (Fig. 13), the spectrum of a s–d shell nucleus (^{21}Ne,

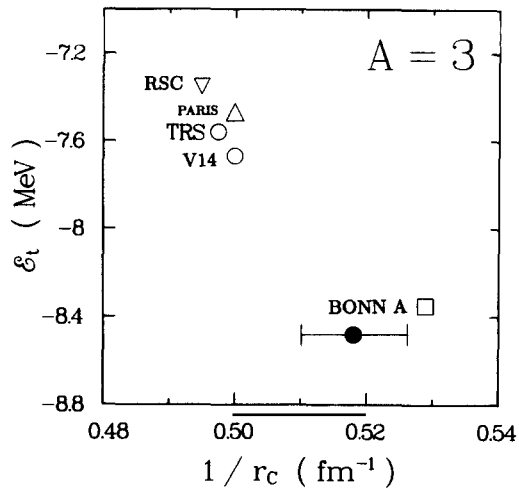

Fig. 13. Triton energy, $\mathscr{E}_t$, versus the invers charge radius of ^{3}He, $1/r_c$, as predicted by various NN potentials. The experimental value is given by the horizontal error bar.

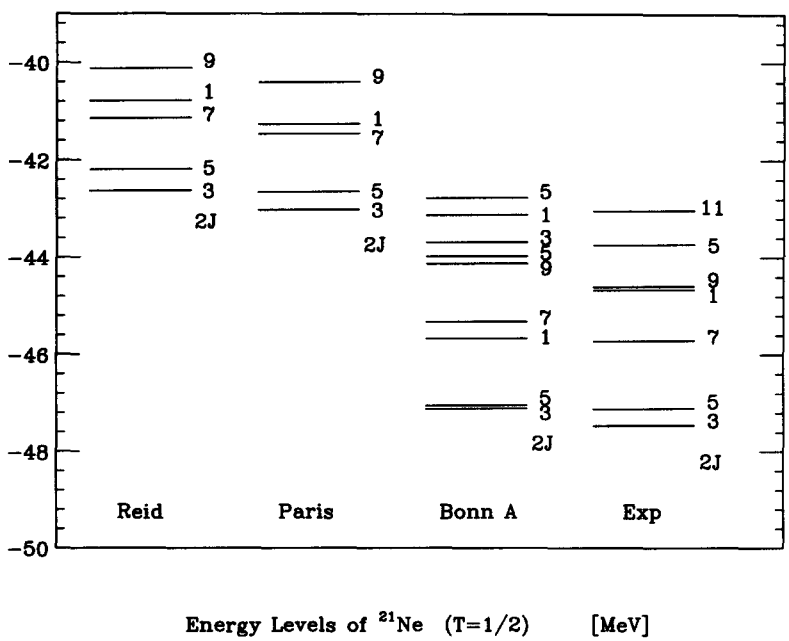

Fig. 14. The spectrum of ^{21}Ne. Predictions by NN potentials are compared with experiment. (From Ref. [37].)

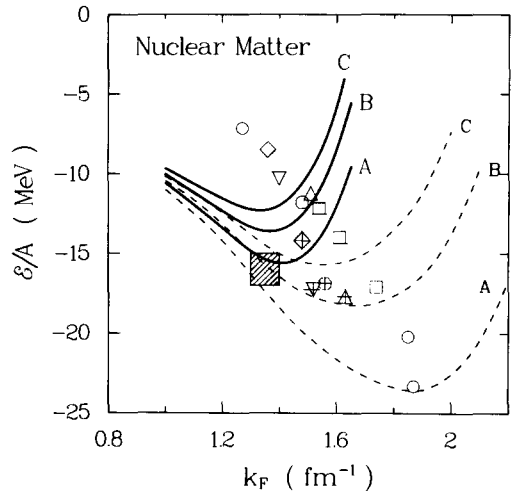

Fig. 15. Energy per nucleon in nuclear matter, $\mathcal{E}/A$, versus density expressed in terms of the Fermi momentum k_F. Dashed lines represent results from non-relativistic Brueckner calculations, while solid lines are Dirac-Brueckner results. The letters *A*, *B*, and *C* refer to the Bonn *A*, *B*, and *C* potential, respectively. The shaded square covers empirical information on nuclear saturation. Symbols in the background denote saturation points obtained for a variety of NN potentials applied in conventional many-body theory. (From Ref. [38].)

Table 5. D-state probability of the deuteron, P_D, as predicted by various potential applied in Figs. 13–15

Potential	P_D (%)
Bonn *A* [6]	4.4
Bonn *B* [6]	5.0
Bonn *C* [6]	5.6
Paris [14]	5.8
TRS [7]	5.9
Argonne V_{14} [8]	6.1
Reid (RSC) [5]	6.5

Fig. 14), and nuclear matter (Fig. 15). To obtain an idea of the strength of the tensor-force component of the various potentials applied, we list P_D in Table 5[8].

The three examples suggest that potentials with weak tensor force (as implied by relativistic meson theory) may be superior in explaining nuclear structure phenomena.

[8] The Bonn *A* potential that occurs in some of the figures is a variation of Bonn *B* with an even weaker tensor force, but otherwise very similar to Bonn *B*. Predictions by Bonn *A* are slightly more attractive as compared to Bonn *B*, but the difference is not substantial; e.g. for the triton binding energy Bonn *B* predicts 8.1 MeV while Bonn *A* yields 8.3 MeV.

5. Summary and conclusions

We have described the developments in the field of realistic NN interactions since the event of the Kuo–Brown matrix elements in 1966. It turns out that each of three models for the NN interaction currently in use, represents one decade of the past 30 years. The Nijmegen potential [13] is an excellent example for approaches typical for the 1960s, the Paris potential a representative of the 1970s, and the Bonn full model for the 1980s. Moreover, we could clearly reveal that with the development of more consistent and comprehensive meson-models over that period of time the quantitative explanation of the NN data has continuously improved. This fact is one of the simplest and best arguments for the appropriateness of meson models in low energy nuclear physics.

We have also taken this opportunity to correct some misconceptions concerning the question of how to test the quantitative nature of NN potentials. Of particular importance is: *predictions by* pp *potentials must only be compared with* pp *data, while predictions by* np *potentials must only be compared with* np *data.* Following this rule, the χ^2/datum for the fit of the relevant world NN data (as obtained by independent researchers in the field [25]) comes out to be 5.1, 3.7, and 1.9 for the Nijmegen [13], Paris [14], and Bonn [15] potential, respectively (cf. Table 1).

Furthermore, we have investigated the influence that differences between different NN potentials have on nuclear structure predictions. It turns out that for potentials that fit the NN data reasonably well, on-shell differences have only a negligible effect. However, potentials that are essentially identical on-shell, may differ substantially off-shell. Such off-shell differences may lead to large differences in nuclear structure predictions. Relativistic, meson-theory based potentials (which are non-local) are in general weaker off-shell than their local counterparts. In particular, the weaker (off-shell) tensor force component (as quantified by a small deuteron D-state probability, P_D) leads to more binding in finite nuclei. For several examples shown, these predictions compare favourably with experiment.

Happy Birthday to Tom Kuo! Our present for Tom is Fig. 14 which shows that the predictive power of the Kuo–Brown approach is even better than anticipated some 25 years ago; last but not least, this is due to progress in our understanding of the nuclear force.

Acknowledgement

It is a pleasure to thank F. Sammarruca for suggestions on the manuscript. This work was supported in part by the U.S. National Science Foundation under Grant Nos. PHY-8911040 and PHY-9211607, and by the Idaho State Board of Education.

Appendix. The proton–proton phase-shifts of the Bonn full model

In the basic paper about the Bonn full model [15], only neutron–proton (np) phase shifts are listed (Table 2 of Ref. [15]). The reason for this is the fact that modern phase-shift analyses [23, 16] state their results in terms of np phase shifts – for practical reasons: the np system exists for all ($T = 0$ and $T = 1$) partial waves and, thus, with np one can cover all cases. In contrast, pp is

Table 6
Proton–proton phase shifts (in degrees) as predicted by the Bonn full model [15]

E_{lab} (MeV)	25	50	100	150	200	300
$^1S_0$	48.309	38.315	23.860	13.298	4.823	−8.288
$^3P_0$	9.209	12.633	10.978	6.223	0.923	−9.349
$^3P_1$	−4.954	−8.295	−13.120	−17.327	−21.406	−29.506
$^1D_2$	0.692	1.677	3.700	5.555	6.998	8.334
$^3P_2$	2.371	5.662	10.945	14.117	15.866	17.238
$^3F_2$	0.104	0.339	0.804	1.138	1.282	0.900
ε_2	−0.822	−1.751	−2.743	−2.987	−2.875	−2.276
$^3F_3$	−0.230	−0.700	−1.564	−2.199	−2.662	−3.318
$^1G_4$	0.039	0.153	0.421	0.690	0.967	1.561
$^3F_4$	0.019	0.100	0.415	0.860	1.366	2.393
$^3H_4$	0.004	0.025	0.108	0.214	0.327	0.539
ε_4	−0.048	−0.195	−0.548	−0.863	−1.122	−1.482

This table lists only a small selection of partial-waves and energies. The pp phase-shifts of the Bonn full model for any energy in the range 10–325 MeV and any partial wave with $J \leq 7$ can be obtained from SAID [25].

restricted to the $T = 1$ two-nucleon states. As explained in detail in Section 3, from the way phase-shift analyses are conducted it is clear that a potential that fits the np phase shifts well, will automatically also fit the pp phase shifts well, *after two minor (but obvious) adjustments are done for the* pp *case*: inclusion of the Coulomb force and fit of the pp singlet scattering length (instead of its np value). Therefore, a potential which has been tested successfully in np does not necessarily have to be tested also in pp. The successful description of also the pp data can be anticipated.

To prove this point, one has to calculate the pp phase shifts correctly. In this appendix, we will do this for the Bonn full model [15]. Since a first calculation [39] of the Bonn pp phase shifts contains some errors, let us stress the important points of the pp phase shift calculation:

(1) In the scattering equation, the correct proton mass of 938.272 MeV is used (and not the average nucleon mass of 938.926 MeV appropriate for np).

(2) The improved, relativistic Coulomb potential [40, 41] is applied[9] (and not the static Coulomb potential).[10]

(3) The $^1S_0$ scattering length is fit to its experimental pp value of $a_{pp}^C = -7.8197$ fm (cf. Table 2) by changing the coupling constant of the σ' contribution to 5.6037 (for np scattering, 5.6893 is used [15]). The effective range parameter turns out to be $r_{pp}^C = 2.7854$ fm, in good agreement with the empirical value (cf. Table 2). This refit is used only for $^1S_0$; the other pp partial waves are kept unchanged as compared to the np case, except for the Coulomb effect. This is the most reasonable assumption, unless one derives all charge-dependent effects accurately from the underlying meson model, which is not our intention here (it is an interesting and comprehensive project for the future).

[9] See Eqs. (25), (26), and (10) of Ref. [27]; in the notation of Ref. [27], we use V_{C1} for the Coulomb potential.

[10] The authors like to thank Dr. Vincent Stoks for drawing their attention to the improved Coulomb potential of Ref. [41].

The pp phase shifts obtained from this calculation (in which the momentum-space method of Ref. [42] is applied[11]) are listed in Table 6. Calculating the pp observables from these phase shifts and comparing with the world pp data, yields a χ^2/datum of 1.94 (cf. Table 1). The χ^2/datum for the corresponding world np data is 1.87 (using the np version of the Bonn full model). This confirms our statement that a potential that fits pp well will automatically also fit np well (*if the proper* pp *phase shifts are used*).

References

[1] T.T.S. Kuo and G.E. Brown, Nucl. Phys. 85 (1966) 40.
[2] T.T.S. Kuo, S.Y. Lee and K.F. Ratcliff, Nucl. Phys. A 176 (1971) 65.
[3] J. Shurpin, T.T.S. Kuo and D. Strottman, Nucl. Phys. A 408 (1983) 310.
[4] T. Hamada and I.D. Johnston, Nucl. Phys. 34 (1962) 382.
[5] R.V. Reid, Ann. Phys. (N.Y.) 50 (1968) 411.
[6] R. Machleidt, Adv. Nucl. Phys. 19 (1989) 189.
[7] R. de Tourreil, B. Rouben and D.W.L. Sprung, Nucl. Phys. A 242 (1975) 445.
[8] R.B. Wiringa, R.A. Smith and T.L. Ainsworth, Phys. Rev. C 29 (1984) 1207.
[9] S. Deister, M.F. Gari, W. Krümpelmann and M. Mahlke, Few-Body Systems 10 (1991) 1.
[10] F. Gross, J.W. van Orden and K. Holinde, Phys. Rev. C 45 (1992) 2094.
[11] H. Kohlhoff, M. Küker, H. Freitag and H.V. von Geramb, in: Proc. 2nd Int. Conf. on Particle Production near Threshold, Uppsala, Sweden, 1992; Physica Skripta 48 (1993) 238.
[12] R. Bryan and B.L. Scott, Phys. Rev. 177 (1969) 1435.
[13] M.M. Nagels, T.A. Rijken and J.J. de Swart, Phys. Rev. D 17 (1978) 768.
[14] M. Lacombe, B. Loiseau, J.M. Richard, R. Vinh Mau, J. Côté, P. Pirès and R. de Tourreil, Phys. Rev. C 21 (1980) 861.
[15] R. Machleidt, K. Holinde and Ch. Elster, Phys. Reports 149 (1987) 1.
[16] R.A. Arndt, J.S. Hyslop III and L.D. Roper, Phys. Rev. D 35 (1987) 128.
[17] A. Gersten, R. Thompson and A.E.S. Green, Phys. Rev. D 3 2076 (1971); G. Schierholz, Nucl. Phys. B 40 (1972) 335; K. Erkelenz, Phys. Rep. 13 C (1974) 191; K. Holinde and R. Machleidt, Nucl. Phys. A 247 (1975) 495; K. Holinde and R. Machleidt, Nucl. Phys. A 256 (1976) 479; J. Fleischer and J.A. Tjon, Nucl. Phys. B 84 (1975) 375, Phys. Rev. D 24 (1980) 87.
[18] J. Sowinski et al., Phys. Lett. 199 B (1987) 341.
[19] D. Bandyopadhyay et al., Phys. Rev. C 40 (1989) 2684.
[20] M. Chemtob, J.W. Durso and D.O. Riska, Nucl. Phys. B 38 141 (1972); A.D. Jackson, D.O. Riska and B. Verwest, Nucl. Phys. A 249 (1975) 397; G.E. Brown and A.D. Jackson, The Nucleon–Nucleon Interaction (North-Holland, Amsterdam, 1976).
[21] R. Vinh Mau, J.M. Richard, B. Loiseau, M. Lacombe and W.N. Cottingham, Phys. Lett. B 44 (1973) 1; R. Vinh Mau, in: Mesons in Nuclei, eds. M. Rho and D.H. Wilkinson (North-Holland, Amsterdam, 1979) p. 151.
[22] J.W. Durso, A.D. Jackson and B.J. VerWest, Nucl. Phys. A 345 (1980) 471.
[23] R.A. Arndt et al., Phys. Rev. D 28 (1983) 97.
[24] R. Dubois et al., Nucl. Phys. A 377 (1982) 554.
[25] R.A. Arndt and L.D. Roper, Scattering Analysis Interactive Dial-in Program (SAID), Virginia Polytechnic Institute and State University, status of September 1992; for information on SAID and how to access it, see reference [40] of R.A. Arndt et al., Phys. Rev. D 45 (1992) 3995.

[11] The authors are indebted to Dr. J. Haidenbauer for some codes involved in the momentum-space Coulomb problem.

[26] G. Piepke, Helvetica Physica Acta 58 (1985) 1049.
[27] J.R. Bergervoet et al., Phys. Rev. C 38 (1988) 15.
[28] O. Dumbrajs et al., Nucl. Phys. B 216 (1983) 277.
[29] D.V. Bugg, Phys. Rev. C 41 (1990) 2708.
[30] R. Blankenbecler and R. Sugar, Phys. Rev. 142 (1966) 1051.
[31] J.J. de Swart, T.A. Rijken, P.M. Maessen and R.G.E. Timmermans, Nuovo Cimento 102 A (1989) 203.
[32] V.G.J. Stoks and J.J. de Swart, Phys. Rev. C 47 (1993) 761.
[33] V.G.J. Stoks, R.A.M. Klomp and J.J. de Swart, unpublished.
[34] J.L. Friar, B.F. Gibson and G.L. Payne, Phys. Rev. C 37 (1988) 2869.
[35] J.L. Friar, Invited Talk at the Theory Institute on The Nuclear Hamiltonian and Electromagnetic Current for the 90s, Argonne, IL, 1991; quoted in: S.A. Coon and M.T. Peña, Proc. XIIIth European Conference on Few-Body Problems, Elba, Italy, 1991, Few-Body Systems, Suppl. 6 (1992) 242.
[36] Sromicki, Phys. Rev. Lett. 57 (1986) 2359.
[37] M.F. Jiang, R. Machleidt, D.B. Stout and T.T.S. Kuo, Phys. Rev. C 46 (1992) 910.
[38] R. Brockmann and R. Machleidt, Phys. Rev. C 42 (1990) 1965.
[39] J. Haidenbauer and K. Holinde, Phys. Rev. C 40 (1989) 2465.
[40] G. Breit, Phys. Rev. 99 (1955) 1581.
[41] G.J.M. Austen and J.J. de Swart, Phys. Rev. Lett. 50 (1983) 2039; G.J.M. Austen, Ph.D. Thesis, Nijmegen 1982, unpublished.
[42] C.M. Vincent and S.C. Phatak, Phys. Rev. C 10 (1974) 391.